Carnegie Observatories Astrophysics Series, Vol. 4:
Origin and Evolution of the Elements, 2004
ed. A. McWilliam and M. Rauch (Cambridge: Cambridge Univ. Press)

Stellar Winds of Hot Massive Stars Nearby and Beyond the Local Group

FABIO BRESOLIN and ROLF P. KUDRITZKI
Institute for Astronomy, University of Hawaii

Abstract

Photospheric radiation momentum is efficiently transferred by absorption through metal lines to the gaseous matter in the atmospheres of massive stars, sustaining strong winds and mass loss rates. Not only is this critical for the evolution of such stars, it also provides us with diagnostic UV/optical spectral lines for the determination of mass loss rates, chemical abundances, and absolute stellar luminosities. We review the mechanisms that render the wind parameters sensitive to the chemical composition, through the statistics of the wind-driving lines. Observational evidence in support of the radiation-driven wind theory is presented, with special regard to the wind momentum-luminosity relationship and the blue supergiant work carried out by our team in galaxies outside of the Local Group.

1.1 A Portrait of Mass Loss in Hot Stars

All stars in the upper Hertzsprung-Russell (H-R) diagram, above $\sim 10^4 L_\odot$, are affected by mass loss via stellar winds (Abbott 1979). Although this statement includes stars in different evolutionary stages [O and B main sequence stars, blue and red supergiants, Wolf-Rayet stars, luminous blue variables (LBVs)], this review will focus on a subset of the "hot" ($T_{\rm eff} \gtrsim 8000$ K) objects, namely OB main sequence and blue supergiant stars. In the corresponding regime of luminosity and effective temperature the radiation field from the stellar photosphere is strong enough to be able to sustain powerful winds, by transfer of photon momentum to the metal ions present in the stellar outer layers. In spite of the low concentration of these ions, when compared to H and He, the momentum is efficiently distributed to the plasma by Coulomb interactions, so that the entire stellar envelope is being accelerated during this process (Springmann & Pauldrach 1992). It is intuitive that the chemical composition and overall metallicity of the stellar outer layers must play a crucial role in determining the strength of the winds and the rate of mass loss.

The basic description given above is the essence of the radiation-driven wind theory, developed during the course of the last 30 years in a number of landmark papers. Following the first suggestion by Lucy & Solomon (1970) concerning the absorption of radiation in the ultraviolet resonance lines of ions such as C IV, Si IV, and N V, recently detected at the time as P Cygni profiles from rocket experiments, the mechanism of wind acceleration by metal-line absorption has been developed further by Castor, Abbott, & Klein (1975) to include the approximate effect of a larger number of strong and weak metal lines. The theoretical framework has subsequently been perfected by the works of Abbott (1982) and Pauldrach, Puls, & Kudritzki (1986). Approximate analytical solutions for velocity fields and mass loss rates within this framework have been developed by Kudritzki et al. (1989). State-of-the-art modeling techniques attain nowadays a realistic description of radiation-driven winds, by solving the radiation transfer of millions of lines in an expanding atmosphere, producing synthetic spectra that match the observations of hot stars from the far-UV to the near-IR to a good degree of accuracy (Hillier & Miller 1998; Pauldrach, Hoffmann, & Lennon 2001; Puls et al. 2003).

1.1.1 Scale of the Phenomenon

Based mainly on IR or radio excess and Hα emission measurements, quite a broad range in the mass loss rate, $\dot{M}$, has been found among hot stars, scaling roughly with stellar luminosity as $L^{1.8}$ (Garmany & Conti 1984; de Jager, Nieuwenhuijzen, & van der Hucht 1988) during the main sequence and the supergiant phase (it is actually the modified wind momentum that scales with some power of the luminosity, as described later). Typical values up to a few times $10^{-6} M_\odot\,\mathrm{yr}^{-1}$ are found among such stars. Wolf-Rayet stars possess denser winds, with mass loss rates up to one order of magnitude higher than O stars, while even more extreme values, up to $10^{-3} M_\odot\,\mathrm{yr}^{-1}$, can be found among LBVs. For central stars of planetary nebulae, $\dot{M} \approx 10^{-7} - 10^{-9} M_\odot\,\mathrm{yr}^{-1}$, by virtue of their lower luminosities (see the recent review by Kudritzki & Puls 2000 for further information on stellar wind properties).

Evidently such rates of mass loss profoundly influence the evolution of massive stars (Chiosi & Maeder 1986). Moreover, winds from massive stars are relevant for the calculation of chemical yields and their inclusion in chemical evolution models of galaxies (Maeder 1992; Portinari, Chiosi, & Bressan 1998). Stellar rotation has also been shown to significantly affect the evolution of massive stars, in particular by enhancing mass loss rates and modifying the surface and wind chemical composition (Meynet & Maeder 2000). An example of recent evolutionary models for massive stars is shown in Figure 1.1, where the solar-metallicity tracks of Meynet & Maeder (2000) for an initial rotational velocity of 300 $\mathrm{km\,s^{-1}}$ are shown for $M = 40 M_\odot$ and $60 M_\odot$. Along the $40 M_\odot$ track the stellar mass and the N/C ratio are indicated at several stages of evolution.

1.2 Why Do Stellar Winds Depend on Metallicity?

Within the galaxies of the Local Group the metallicity varies by more than one order of magnitude, from metal-poor dwarf irregulars such as WLM to metal-rich giant spirals such as M31, offering the opportunity to probe the effects of chemical abundances on the character of the stellar winds. Expanded possibilities have appeared with the advent of 8–10 meter telescopes, which allow us to extend the spectroscopic study of individual stars even beyond the Local Group. Quantitative stellar spectroscopy in external galaxies is becoming important for a number of projects dealing with stellar abundances, the distance scale, the evolution of massive stars, the characterization of supernova progenitors, and the instabilities of massive stars in the very upper part of the H-R diagram, near the Humphreys-Davidson (1979) limit. The work carried out within our group is mostly concerned with the first two aspects. For the distance scale work, see the recent review by Bresolin (2004). Here we will succinctly illustrate how current observations of hot stars compare with the theoretical predictions concerning their stellar winds.

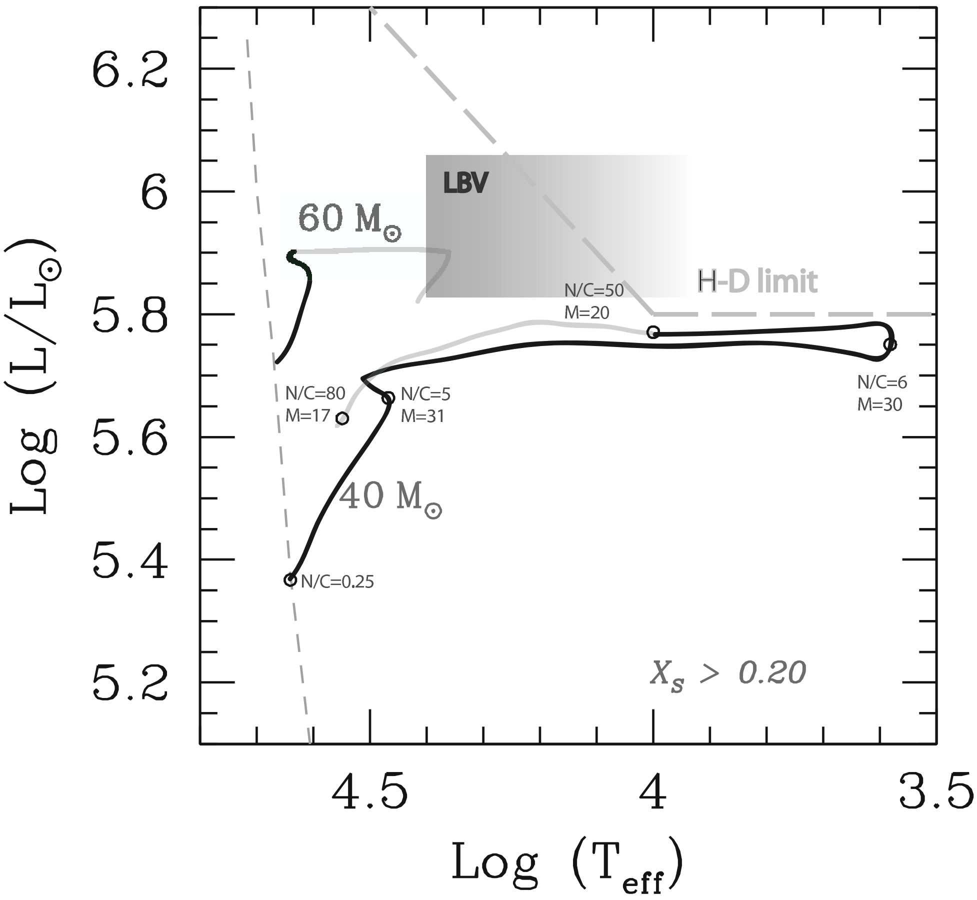

Fig. 1.1. Schematic H-R diagram showing the rotating ($V_\mathrm{i} = 300\,\mathrm{km\,s^{-1}}$) solar metallicity $40\,M_\odot$ and $60\,M_\odot$ stellar tracks from Meynet & Maeder (2000). For clarity the tracks are plotted up to the point at which the fractional hydrogen mass at the surface $X_S = 0.2$. The early WN phase is plotted in gray. The ZAMS location (short-dashed line) and the Humphreys-Davidson limit (long-dashed line) are shown, together with the typical location of LBV stars (shaded area). At several positions along the $40\,M_\odot$ track the stellar mass and the surface N/C ratio are reported.

1.2.1 Theoretical Landscape

As briefly mentioned in the previous section, the winds of hot massive stars are well described within the framework of the radiation-driven theory. For more details and references on the subject, the interested reader is referred to the reviews by Kudritzki (1998) and Kudritzki & Puls (2000).

Let us consider a hot and massive star radiating a total luminosity L out of its photosphere. The outer layers will be accelerated by radiation pressure through absorption in the metal lines. The maximum total momentum available from the radiation field is L/c, so that we can expect a dependence of the mechanical momentum flow:

$$\dot{M}v_\infty = f(L/c). \tag{1.1}$$

As a result of this transfer of momentum from the radiation to the ions, the wind is accelerated, starting from the photospheric layers, up to the asymptotic terminal velocity υ_∞. The observed stellar wind velocity fields are customarily parameterized as a "β-law," given here in its simplest form:

$$\upsilon(r) = \upsilon_\infty \left(1 - \frac{R_\star}{r}\right)^\beta . \tag{1.2}$$

For the hot O stars, $\beta \simeq 0.8$, and therefore the ions are efficiently accelerated right above the photosphere, while for later-type A supergiants a more progressive acceleration takes place, corresponding to $\beta \simeq 2-4$.

When considering the hydrodynamics of a stationary line-driven wind, we start from the fundamental equations describing the conservation of mass

$$\dot{M} = 4\pi r^2 \rho \upsilon, \tag{1.3}$$

where $\rho = \rho(r)$ is the local density, together with the equation of motion

$$\upsilon \frac{d\upsilon}{dr} = -\frac{1}{\rho}\frac{dP_{\rm gas}}{dr} - g + g_{\rm rad}, \tag{1.4}$$

where the radiative acceleration $g_{\rm rad}$ can be expressed as the sum

$$g_{\rm rad} = g_{\rm rad}^{\rm Th} + g_{\rm rad}^{\rm lines} + g_{\rm rad}^{\rm ff,bf}. \tag{1.5}$$

Of these three terms, only the second one (the acceleration due to line absorption) needs to be considered in more detail, the first one (Thomson scattering) will be included as a constant reduction of the gravity g, whereas the third one (free-free + bound-free transitions) is negligible in the winds of hot stars.

Since the work by Castor et al. (1975) and Pauldrach et al. (1986), the radiative term of the line acceleration is parameterized in terms of a *line force multiplier*, $M(t)$, such that

$$g_{\rm rad}^{\rm lines} = CF\; g_{\rm rad}^{\rm Th}\, M(t), \tag{1.6}$$

with CF being the correction factor that accounts for the finite extension of the stellar disk. The optical depth parameter t, multiplied by the dimensionless line strength k (i.e. the line opacity divided by the Thomson opacity $n_e\sigma_e$; see Kudritzki & Puls 2000), gives the optical depth in a given line transition in a supersonically expanding atmosphere:

$$\tau = kt \tag{1.7}$$

$$t = n_e \sigma_e \frac{\upsilon_{\rm therm}}{d\upsilon/dr}. \tag{1.8}$$

In its simplest form (see Abbott 1982, Pauldrach et al. 1986, and Kudritzki 2002 for a more accurate description) the line force multiplier is then expressed as

$$M(t) \propto N_{\rm eff}\, t^{-\alpha}, \tag{1.9}$$

thus depending on the effective number of metal lines driving the wind, $N_{\rm eff}$, and on the optical depth through the line force parameter α. Solving the equation of motion (Eq. 1.4) with this parameterization of the line force, one obtains scaling relations for the mass loss rate and the terminal velocity (Kudritzki et al. 1989):

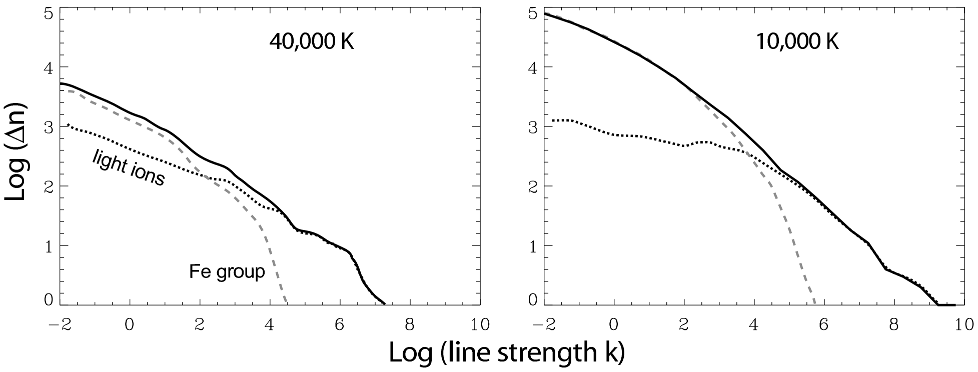

Fig. 1.2. Line distribution functions for $T_{\rm eff} = 40{,}000$ K (*left*) and $T_{\rm eff} = 10{,}000$ K (*right*) and solar composition, plotted separately for iron-group elements (dashed lines) and lighter ions (dotted lines). The full line represents the total distribution. (Adapted from Puls et al. 2000.)

$$\begin{aligned} \dot{M} &\approx (N_{\rm eff} L)^{1/\alpha} \left[M_\star(1-\Gamma)\right]^{1-1/\alpha} \\ v_\infty &\approx \frac{\alpha}{1-\alpha} v_{\rm esc}. \end{aligned} \tag{1.10}$$

Note that $M_\star(1-\Gamma)$ is the stellar *effective mass* (which accounts for the ratio Γ of Thomson scattering to gravitational acceleration).

The origin of the $M(t)$ expression used in the proportionality of Equation (1.9) lies in the statistics of the strengths of the wind-driving lines, which can be described by a simple *line strength distribution function*. It is found that, to a good approximation, the number of lines of a given strength k follows a power law (Fig. 1.2):

$$n(k)d(k) \propto k^{\alpha-2} dk \qquad (0 < \alpha < 1; \;\; 1 < k < k_{\rm max}). \tag{1.11}$$

The exponent α, which determines the slope of the distribution function, is mostly set by the laws of atomic physics (the distribution function of oscillator strengths), and is found to vary between 0.5 and 0.7 (for the hydrogen Lyman series one would obtain $\alpha = 2/3$). $N_{\rm eff}$ (see Eqs. 1.9 and 1.10) is related to the normalization of the line strength distribution function. Also note that a power law is only an approximation and that there is a slight curvature in the distribution function.

The line distribution function plays a primary role in the mechanisms governing radiation-driven winds (see Puls, Springmann, & Lennon 2000 for an in-depth study), and it is worthwhile spending a few additional words in relation to the type of ions that are most effective in driving the wind. It is clear that such ions will differ among stars of different chemical composition and/or effective temperatures, since the predominant ionization stages will change accordingly.

What kind of lines are driving the wind? The most prominent metal-line transitions are located in the far-UV and UV spectral ranges. As the emitted stellar flux peaks at lower frequencies with decreasing $T_{\rm eff}$, so does the spectral range containing the lines contributing the most at driving the wind. The calculations by Abbott (1982) and Puls et al. (2000)

show that lines of high-ionization stages of O, N, P, and other heavy elements, located approximately between 800 and 1200 Å, are the dominant source of acceleration in the hottest (40,000 K) stars. At lower temperatures (10,000–20,000 K) lower-ionization species (such as Fe II, Fe III, Mg II, Ca II), having transitions at longer wavelengths, become predominant. The relative importance of CNO, Fe-group, and other elements changes with $T_{\rm eff}$ as well. For solar composition C, N, and O dominate over iron-group elements for $T_{\rm eff} > 25{,}000$ K, and down to lower temperatures as the overall metallicity decreases (Vink, de Koter, & Lamers 2001). As the right panel in Figure 1.2 shows, at lower temperature the number of iron-group lines present, mostly Fe II–III, increases, resulting in a steepening of the line distribution function and a consequent decrease in α.

We can now answer our question regarding the origin of the metallicity dependence of the mass loss, based on the understanding of the line statistics briefly discussed so far. There are two main effects.

(1) To first order, the line strengths of the individual metal lines driving the wind are proportional to metallicity,

$$k \approx \frac{Z}{Z_\odot} k_\odot, \tag{1.12}$$

so that the distribution functions in Figure 1.2 shift horizontally in the plotted log–log plane. Consequently, the normalization over the range $1 < k < k_{\rm max}$ changes with metallicity, affecting the effective number of lines driving the wind:

$$N_{\rm eff} \propto Z^{1-\alpha}. \tag{1.13}$$

(2) There is a metallicity dependence of α, coming from the curvature of the line distribution function, which tends to become steeper at high line strengths (see Puls et al. 2000 for the details). It is important to note that the local acceleration in the wind comes mostly from lines with $\tau \simeq 1$. This means that strong winds are driven by lines with smaller line strengths, whereas weak winds rely on the acceleration of the fewer lines with large line strengths.

To conclude, the predicted scaling relations for the metallicity dependence of the wind parameters, valid approximately in the range $0.1 < Z/Z_\odot < 3$, are

$$\dot{M} \sim Z^{(1-\alpha)/\alpha} = Z^m, \tag{1.14}$$

with $m = 0.5 - 0.8$ for O- and B-type stars, and

$$v_\infty \sim Z^{0.13-0.15} \tag{1.15}$$

(Kudritzki, Pauldrach, & Puls 1987; Leitherer, Robert, & Drissen 1992). While the effects on the mass loss are mostly a direct result of (1) through Equations (1.10) and (1.13), the metallicity dependence of v_∞ is solely caused by (2) and Equation (1.10). At very low metallicities (below $10^{-2} Z_\odot$) these relations break down, and the depth dependence of the line force multipliers must be taken into account (Kudritzki 2002). We also conclude from Figure 1.2 that a change of the relative abundance ratio of α elements to Fe-group elements will have an additional effect.

1.3 Does Nature Conform to Theory?

The first obvious observational test of the effects of metallicity on the stellar winds of massive stars concerns the terminal velocities. These are easily measured from the P Cygni profiles of resonance lines in the UV, such as C IV $\lambda1550$ and Si IV $\lambda1400$. A clear decrease of υ_∞ is found when comparing the terminal velocities measured in the Milky Way with those in the Magellanic Clouds, especially in the lower-metallicity SMC (Garmany & Conti 1985; Kudritzki & Puls 2000). Direct comparisons of O-star P Cygni profiles at high (Galactic) and low (SMC) metallicity can be found, for example, in Leitherer et al. (2001) and Heap, Hubeny, & Lanz (2001).

Concerning the mass loss rates, their derivation is more model dependent. The bulk of the measurements available for massive stars comes from Hα line profile fits. However, when correlating $\dot{M}$ with, for example, the luminosity L, a significant scatter is found, as a consequence of the dependence on the effective mass (see Eq. 1.10). This difficulty vanishes, at least theoretically, when considering the wind momentum through Equation (1.10), since $\upsilon_{\rm esc}$ depends on the square root of the effective gravitational potential:

$$\dot{M}\upsilon_\infty \propto \frac{(N_{\rm eff}\,L)^{1/\alpha}}{R_\star^{0.5}}\left[M_\star(1-\Gamma)\right]^{3/2-1/\alpha}. \tag{1.16}$$

The fortuitous nulling of the exponent for the effective mass (since $\alpha \simeq 2/3$ for hot stars) then relates the *modified wind momentum*

$$D_{\rm mom} = \dot{M}\upsilon_\infty(R_\star/R_\odot)^{0.5} \tag{1.17}$$

to the stellar luminosity in a simple wind momentum-luminosity relationship (WLR)

$$\log D_{\rm mom} = a + b\log\frac{L}{L_\odot} \tag{1.18}$$

(see Kudritzki 1988 or Kudritzki & Przybilla 2004 for a recent detailed derivation), which constitutes the basis of our program to use the winds of massive stars in external galaxies to determine their distances. [An independent method valid for blue supergiants, the flux-weighted gravity-luminosity relationship (FGLR) has been recently proposed by Kudritzki, Bresolin, & Przybilla (2003).]

From Equation (1.16), it is evident that a and $b = 1/\alpha$ in Equation (1.18), which are to be derived from observations for an empirical WLR, are a function of the predominant ionization stages in the stellar atmosphere (spectral type) and of the metallicity. The slope and zero-point of the WLR are, in fact, found to differ for O, B, and A supergiant stars by Kudritzki et al. (1999), as illustrated in Figure 1.3.

Combining the metallicity effect on $\dot{M}$ and υ_∞ discussed in the previous section, the theoretical dependence of the modified wind momentum on metallicity becomes

$$D_{\rm mom} \sim Z^{0.6-0.8}. \tag{1.19}$$

Puls et al. (1996) and Herrero, Puls, & Najarro (2002) have shown that the Galactic O stars follow the WLR predicted by the radiation-driven theory rather convincingly. Data on B and A supergiants, as well as on lower-metallicity massive stars that would allow a test of Equation (1.19), remain scant. Puls et al. (1996) indeed found a decrease in the wind momentum for a small sample of O stars in the Magellanic Clouds compared to similar stars in the Milky Way, in rough agreement with the theoretical expectations. Vink et al. (2001)

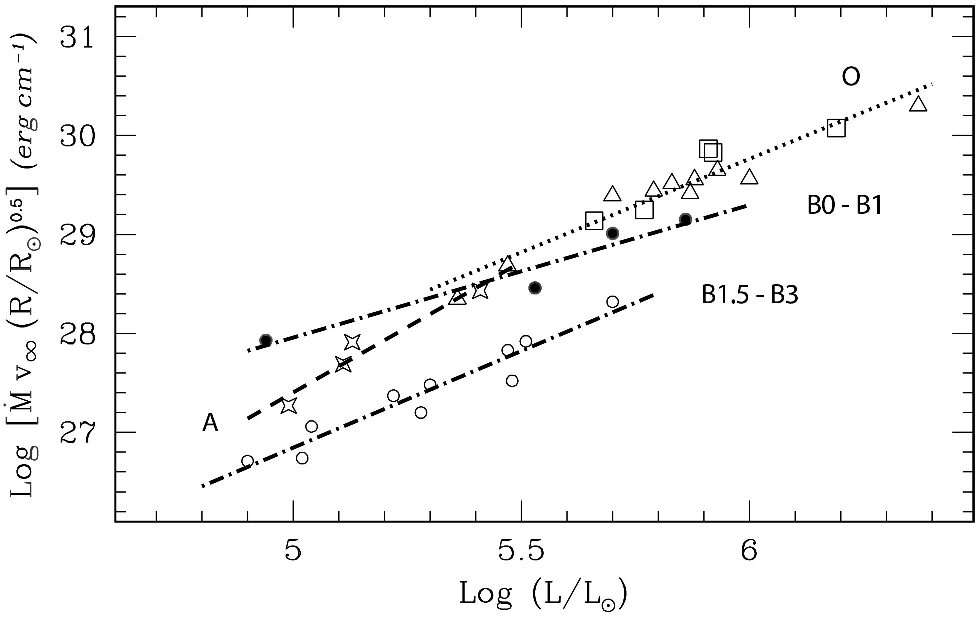

Fig. 1.3. Spectral type dependence of the WLR for Galactic supergiant stars. Different symbols are used for different spectral type ranges, and the corresponding linear regression lines are drawn. (Adapted from Kudritzki et al. 1999.)

have also found reasonable agreement between predicted and observed mass loss rates of O-type stars in the LMC and SMC, if the adopted metallicity is $0.8\,Z_\odot$ and $0.1\,Z_\odot$, respectively.

1.4 Looking Beyond the Local Group

Among the most exciting developments in stellar research in recent years has been the possibility of quantitative studies of individual stars in external galaxies located even beyond the Local Group, thanks to observations with 8 m-class telescopes. When working at $V \simeq 19-20$ mag or fainter in a galaxy several Mpc away, the natural targets become the visually brightest mid-B to early-A supergiants and hypergiants (with the occasional LBV). Reaching absolute magnitudes $M_V \simeq -8$ to -9, they can be studied spectroscopically out to $10-15$ Mpc. Such stars hold the promise of delivering important information on stellar abundance patterns, a welcome complement to H II region studies, and extragalactic distances (via the WLR and the FGLR) even at a moderate spectral resolution of $R \simeq 1000-2000$.

Pioneering results concerning quantitative stellar spectroscopy at such distances have been obtained recently within our collaboration, taking advantage of the multi-spectrum capabilities offered at the Very Large Telescope with the FORS instrument. Supergiant stars in NGC 3621, a late-type spiral with a Cepheid distance of 6.7 Mpc studied by Bresolin et al. (2001), remain the farthest *normal* stars for which information regarding the stellar wind and abundances have been obtained so far. The non-LTE spectral synthesis of two A-type supergiants in NGC 3621 reveals a sub-solar overall metallicity (Bresolin et al. 2001; Przy-

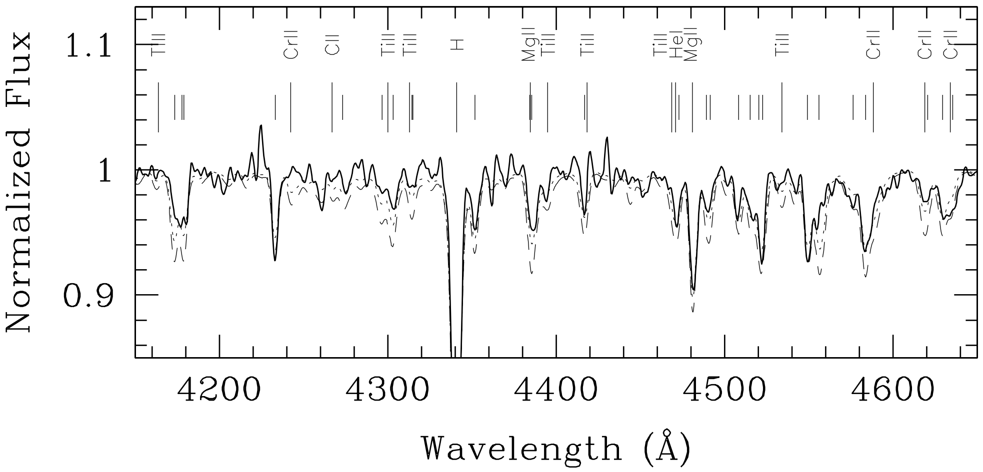

Fig. 1.4. Portion of the rectified blue VLT/FORS spectrum of an A0 Ia star in NGC 300. Principal spectral lines are identified at the top. Synthetic models are shown for $Z = Z_{\odot}$ (dashed line) and $Z = 0.5\,Z_{\odot}$ (dotted line).

billa 2002) and indicates that the internal accuracy in abundance, even at the moderate FORS resolution, is ~ 0.2 dex.

Additional blue supergiants have been investigated spectroscopically in NGC 300, at a distance of 2 Mpc, by Bresolin et al. (2002a). This work is part of a larger project aimed at improving the accuracy of stellar candles used to measure distances of nearby galaxies. The study of the blue supergiants, in particular, will provide stellar chemical compositions needed to test the Cepheid period-luminosity relation at varying metallicities, and at the same time independent distances to the parent galaxies via the WLR and the FGLR, once calibrated in nearby galaxies (Bresolin 2004).

The abundance diagnostic power of the A supergiant VLT spectra in NGC 300 is illustrated in Figure 1.4, where $Z/Z_{\odot} \simeq 0.5$ is derived for an A0 Ia star from a comparison with synthetic spectra. A similar work has been carried out for early B-type supergiants from the same set of spectra by Urbaneja et al. (2003). This allows us a comparison between stellar and nebular abundances in NGC 300, using published results on the O/H abundance of H II regions (Deharveng et al. 1988) and adopting [O/H]=[M/H] for A stars, where M/H is the mean stellar metallicity (Fig. 1.5).

Only for very few external spiral galaxies has such a kind of comparison been carried out so far, namely the Local Group members M33 (Monteverde et al. 1997; Monteverde, Herrero, & Lennon 2000) and M31 (Smartt et al. 2001; Venn et al. 2001; Trundle et al. 2002; see also the contribution by Venn et al. 2004 on dwarf irregular galaxies at this conference). However, the importance of such comparisons cannot be overstated, because of the need for a check on the nebular abundances, which in the case of most spiral galaxies rely on empirical “strong line” methods, which can contain systematic errors on the estimated abundances amounting to factors of 2 or 3 (Kennicutt, Bresolin, & Garnett 2003). While the result for NGC 300 is still very preliminary, and based on a small number of stars, it

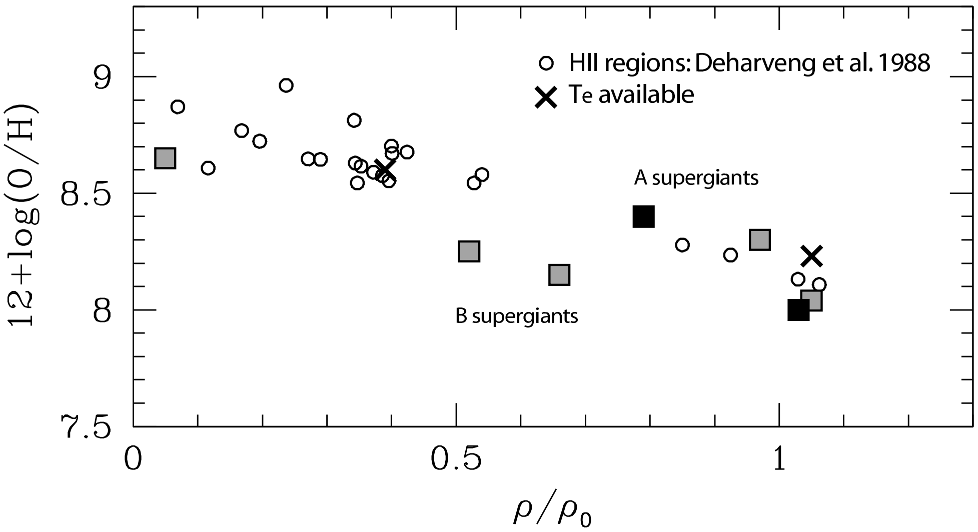

Fig. 1.5. Preliminary comparison of the nebular (circles) and stellar (squares) abundance gradients derived for NGC 300, expressed in terms of the fractional isophotal radius. The H II region abundances have been estimated from the semi-empirical $R_{23} = ([\mathrm{O\,II}] + [\mathrm{O\,III}])/\mathrm{H}\beta$ calibration by Kobulnicky, Kennicutt, & Pizagno (1999), except for two regions (crosses), for which a direct abundance determination has been made possible.

suggests a rough agreement between stars and H II regions, even though the O/H scale for the latter is dependent upon which empirical calibration one chooses to adopt.

1.4.1 Stellar Winds in Supergiants Outside the Local Group

High-resolution studies of individual blue supergiants outside of the Milky Way and the Magellanic Clouds have been made in M33 (McCarthy et al. 1995), M31 (McCarthy et al. 1997; Venn et al. 2000), NGC 6822 (Venn et al. 2001), and WLM (Venn et al. 2003). The winds of some of these stars have also been analyzed, and their strength roughly corresponds with the theoretical expectations, based on the measured luminosities and abundances. However, a systematic investigation of the wind properties of a sizable sample of blue supergiants in a single galaxy has yet to come. This is necessary for understanding the parameters affecting the strength of stellar winds, in particular their dependence on metallicity. The NGC 300 supergiant sample presented by Bresolin et al. (2002a), soon to be complemented by objects observed at the VLT in another Sculptor member, NGC 7793, gives us the chance to partly remedy the situation, although at such distances lower spectral resolutions must be used.

Six A supergiants in NGC 300 have been analyzed with the unblanketed version of the FASTWIND code described by Santolaya-Rey, Puls, & Herrero (1997) to measure mass loss rates from the Hα line profiles and gravities from Hγ. $\dot{M}$ was found to span the range $1.4 \times 10^{-8} - 2.3 \times 10^{-6} M_{\odot}\ \mathrm{yr}^{-1}$, with luminosities $\log(L/L_{\odot}) = 4.8 - 5.7$ ($M_V = -6.8$ to -8.6 mag).

The resulting WLR is displayed in Figure 1.6, where results for A supergiants in the Milky Way, M31 (Kudritzki et al. 1999), and NGC 3621 (Bresolin et al. 2001) are included. As can be seen, the $D_{\mathrm{mom}} - Z$ scaling relation (§ 1.3) applied to the Galactic regression line for

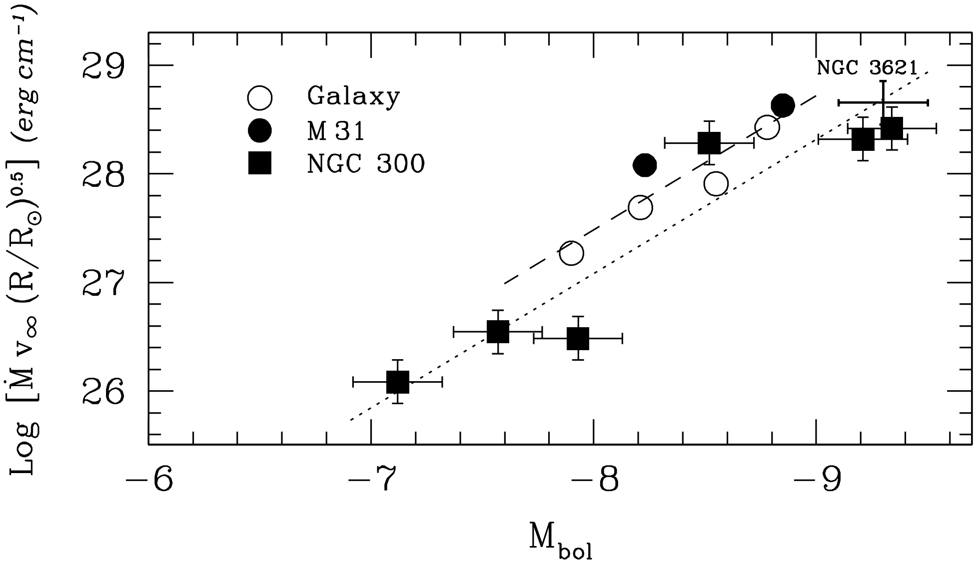

Fig. 1.6. The A-type supergiant WLR, including objects from the Milky Way, M31, NGC 300, and NGC 3621. The linear fit to the Galactic and M31 stars is shown by the dashed line. A theoretical scaling factor is applied to provide the expected relation at $Z/Z_\odot = 0.4$ (dotted line), the mean metallicity found for the NGC 300 and NGC 3621 stars included in the plot.

the mean metallicity of the NGC 300 stars ($Z \simeq 0.4 Z_\odot$, dotted line) provides a reasonable fit to the data. Some discrepancies are present, but our general conclusion is that theory and observations are in fair agreement. The analysis of a larger number of stars, including the effects of blanketing, is needed.

1.5 Multiwavelength Studies

The importance of the multiwavelength approach in the study of massive star winds and abundances has been clearly illustrated by Taresch et al. (1997), who analyzed far-UV (*ORFEUS*), UV (*IUE*) and optical spectra of the Galactic star HD 93129A (recently included in the newly defined O2 If* spectral class by Walborn et al. 2002). While the UV spectral range in general has been much more accessible than the far-UV, the amount of information regarding temperatures and abundances that can be collected from the UV alone is quite limited. Therefore, the iron abundance was estimated to be roughly solar from spectrum synthesis of the plethora of iron lines present in the UV (see Haser et al. 1998 for a similar approach applied to Magellanic Cloud O stars). This result was complemented by the measurement of optical lines to derive CNO abundances (finding a 2 × solar overabundance for N, and a ∼ 5 × depletion for C and O), and by the access to additional ionization stages of several elements (e.g., unsaturated lines of C III, N III–IV, O VI, S VI, P V), which become important in constraining the abundances and stellar effective temperatures, as well as the mass loss rates.

The effectiveness of this technique has been recently demonstrated by Crowther et al. (2002a), who analyzed *FUSE* far-UV wind-affected metal lines of four Magellanic Cloud O supergiants, together with *IUE+HST* UV and optical data. The far-UV spectra have been crucial in fixing the $T_{\rm eff}$'s, which resulted systematically 5000–7000 K lower than determined previously from unblanketed, plane-parallel models (see also Puls et al. 2003; Bianchi & Garcia 2002). Mass loss rates are also substantially revised downwards, as a consequence of lower luminosities. As in the case of HD 93129A studied by Taresch et al., strong N enrichment has been detected, together with modest C depletion, adding another piece of evidence for mixing processes affecting the surface chemical composition of evolved massive stars (see also Lennon, Dufton, & Crowley 2003).

As a final remark, it is worth emphasizing the importance of the modeling techniques used to derive the stellar parameters, currently relying on the full line blanketing and spherical extension treatment in non-LTE of the radiative transfer equation in the expanding atmospheres. Unified model atmosphere codes, such as CMFGEN (Hillier & Miller 1998) and WM-basic (Pauldrach et al. 2001), are now routinely employed to investigate the stellar properties of massive stars.

1.6 Additional Matters

1.6.1 Wolf-Rayet Stars

Wolf-Rayet stars are spectacular manifestations of the profound effects of mass loss on the evolution of massive stars. The removal of the outer layers of the stars progressively reveals, toward the late evolutionary stages, the products of H-burning (WN stars) and, subsequently, He-burning (WC stars). Because of the mechanism responsible for this effect—the transfer of photon momentum to the gas via metal-line absorption—the efficiency of this peeling process is highly dependent on metallicity. First of all, the minimum progenitor mass required for Wolf-Rayet star formation decreases with increasing metallicity (Maeder & Meynet 1994), ranging observationally from 20–25 $M_\odot$ in the Milky Way to 70 $M_\odot$ in the SMC (Massey, De Gioia-Eastwood, & Waterhouse 2000, 2001). Moreover, the WC/WN number ratio, which measures the efficiency of the evaporation process, increases from virtually zero at SMC abundance to almost one at super-solar abundance, as in the case of M31 (Massey 2003).

The high mass loss of Wolf-Rayet stars is manifested by the strong H, He, and metal emission lines present in their spectra. This facilitates their detection with narrow-band "on-off" imaging techniques and provides the spectroscopist with a means to probe detailed chemical abundance patterns in their outer layers, which invariably reflect their advanced evolutionary status. In this regard, besides quantitative work in the Milky Way, the Magellanic Clouds and a few Local Group galaxies (e.g., Herald, Hillier, & Schulte-Ladbeck 2001; Smartt et al. 2001; Crowther et al. 2002b), objects at much larger distances have started to be analyzed. Bresolin et al. (2002b) have presented chemical abundance patterns in a WN11 star they discovered in NGC 300. In this galaxy Schild et al. (2003) list nearly 60 Wolf-Rayet stars, based on a VLT imaging survey, and analyze the spectra of two WC stars. According to these authors there are at least a dozen Wolf-Rayet stars or Wolf-Rayet star candidates brighter than $V \simeq 19$ mag (the magnitude of the WN11 studied by Bresolin et al. 2002b) in this galaxy alone, opening up the possibility for quantitative studies of a large number of emission-line stars outside the Local Group.

1.6.2 Starbursts and the High-redshift Universe

It is of consolation to part of the hot-star community that the same kind of analyses and modeling used for nearby single stars can be successfully used for the understanding of stellar populations and chemical abundances in distant galaxies. Such is the case in the study of starburst events at distances where only the integrated light from a composite stellar population can be measured, where strong UV wind and photospheric lines can help constrain the properties of the emitting regions. Population synthesis models have become popular in order to disentangle several characterizing properties of the star-forming regions, such as the initial mass function, the star formation history, the age, and the chemical abundance. Recent examples of the application of this technique are given by González Delgado et al. (2002) for the metal-rich starburst galaxy NGC 3049, and Leitherer et al. (2001) for NGC 5253. In the latter case the main UV spectral features are reasonably well reproduced by synthetic models based on UV stellar libraries constructed from metal-poor Magellanic Cloud O stars, rather than Galactic ones. A similar result has been obtained by the same authors, as well as by Heap et al. (2001), for the well-known lensed galaxy MS1512–cB58. However, we have already run short of UV stellar templates, as we currently have no other metallicities represented in the synthetic models other than those of the Galactic and the Magellanic Cloud stars. Besides, B stars are included only for the Galactic case. The solution to these difficulties is represented by the use, instead of observed stellar spectra, of model UV spectra, where the metallicity can be varied at will. The reliability of the stellar models must, of course, first be tested against the existing templates. The outcome in the near future will be a better knowledge of the properties, in particular of the chemical abundances, of high-redshift star-forming regions and primordial galaxies.

References

Abbott, D. C 1979, in IAU Symp. 83, Mass Loss and Evolution of O-type Stars, ed. P. S. Conti & C. W. H. de Loore (Dordrecht: Reidel), 237

——. 1982, ApJ, 259, 282

Bianchi, L. & Garcia, M. 2002, ApJ, 581, 610

Bresolin, F. 2004, in Stellar Candles for the Extragalactic Distance Scale, ed. D. Alloin & W. Gieren (Berlin: Springer), in press

Bresolin, F., Gieren, W., Kudritzki, R. P., Pietrzynski, G., & Przybilla, N. 2002a, ApJ, 567, 277

Bresolin, F., Kudritzki, R. P., Mendez, R., & Przybilla, N. 2001, ApJ, 547, 123

Bresolin, F., Kudritzki, R. P., Najarro, F., Gieren, W., & Pietrzynski, G. 2002b, ApJ, 577, L107

Castor, J. I., Abbott, D. C., & Klein, R. I. 1975, ApJ, 195, 157

Chiosi, C., & Maeder, A. 1986, ARA&A, 24, 329

Crowther, P. A., Dessart, L., Hillier, D. J., Abbott, J. B., & Fullerton, A. W. 2002b, A&A, 392, 653

Crowther, P. A., Hillier, D. J., Evans, C. J., Fullerton, A. W., De Marco, O., & Willis, A. J. 2002a, ApJ, 579, 774

Deharveng, L., Caplan, J., Lequeux, J., Azzopardi, M., Breysacher, J., Tarenghi, M., & Westerlund, B. 1988, A&AS, 73, 407

de Jager, C., Nieuwenhuijzen, H., & vander Hucht, K. A. 1988, A&AS, 72, 259

Garmany, C. D., & Conti, P. S. 1984, ApJ, 284, 705

——. 1985, ApJ, 293, 407

González Delgado, R. M., Leitherer, C., Stasińska, G., & Heckman, T. M. 2002, ApJ, 580, 824

Haser, S. M., Pauldrach, A. W. A., Lennon, D. J., Kudritzki, R.-P., Lennon, M., Puls, J., & Voels, S. A. 1998, A&A, 330, 285

Heap, S. R., Hubeny, I., & Lanz, T. M. 2001, Ap&SSS, 277, 263

Herald, J. E., Hillier, D. J., & Schulte-Ladbek, R. E. 2001, ApJ, 548, 932

Herrero, A., Puls, J., & Najarro, F. 2002, A&A, 396, 949

Hillier, D. J., & Miller, D. L. 1998, ApJ, 496, 407

Humphreys, R. M., & Davidson, K. 1979, ApJ, 232, 409

Kennicutt, R. C., Bresolin, F., & Garnett, D. R. 2003, ApJ, 591, 801
Kobulnicky, H. A., Kennicutt, R. C., & Pizagno, J. 1999, ApJ, 514, 544
Kudritzki, R. P. 1998, in Stellar Astrophysics for the Local Group, ed. A. Aparicio, A. Herrero, & F. Sanchez (Cambridge: Cambridge Univ. Press), 149
——. 2002, ApJ, 577, 389
Kudritzki, R. P., Bresolin, F., & Przybilla, N. 2003, ApJ, 582, L83
Kudritzki, R. P., Pauldrach, A., & Puls, J. 1987, A&A, 173, 293
Kudritzki, R. P., Pauldrach, A., Puls, J., & Abbott, D. C. 1989, A&A, 219, 205
Kudritzki, R. P., & Przybilla, N. 2004, in Stellar Candles for the Extragalactic Distance Scale, ed. D. Alloin & W. Gieren (Berlin: Springer), in press
Kudritzki, R. P., & Puls, J. 2000, ARA&A, 38, 613
Kudritzki, R. P., Puls, J., Lennon, D. J., Venn, K. A., Reetz, J., Najarro, F., McCarthy, J. K., & Herrero, A. 1999, A&A, 350, 970
Leitherer, C., Leao, J. R. S., Heckman, T. M., Lennon, D. J., Pettini, M., & Robert, C. 2001, ApJ, 550, 724
Leitherer, C., Robert, C., & Drissen L. 1992, ApJ, 401, 596
Lennon, D. J., Dufton, P. L., & Crowley, C. 2003, A&A, 398, 455
Lucy, L. B., & Solomon, P. M. 1970, ApJ, 159, 879
Maeder, A. 1992, A&A, 264, 105
Maeder, A., & Meynet, G. 1994, A&A, 287, 803
McCarthy, J. K., Kudritzki, R. P., Lennon, D. J., Venn, K. A., & Puls, J. 1997, ApJ, 482, 757
McCarthy, J. K., Lennon, D. J., Venn, K. A., Kudritzki, R. P., Puls, J., & Najarro, F. 1995, ApJ, 455, L135
Massey, P. 2003, ARA&A, 41, 15
Massey, P., De Gioia-Eastwood, K., & Waterhouse, E. 2000, AJ, 119, 2214
——. 2001, AJ, 121, 1050
Meynet, G., & Maeder, A. 2000, A&A, 361, 101
Monteverde, M. I., Herrero, A., & Lennon, D. J. 2000, ApJ, 545, 813
Monteverde, M. I., Herrero, A., Lennon, D. J., & Kudritzki, R. P. 1997, ApJ, 474, L107
Pauldrach, A., Hoffmann, T. L., & Lennon, M. 2001, A&A, 375, 161
Pauldrach, A., Puls, J., & Kudritzki, R. P. 1986, A&A, 164, 86
Portinari, L., Chiosi, C., & Bressan, A. 1998, A&A, 334, 505
Przybilla, N. 2002, Ph.D. Thesis, Ludwig-Maximillians Universitaets
Puls, J., et al. 1996, A&A, 305, 171
Puls, J., Repolust, T., Hoffmann, T., Jokuthy, A., & Venero, R. 2003, in IAU Symp. 212, A Massive Star Odyssey, from Main Sequence to Supernova, ed. K. A. van der Hucht, A. Herrero, & C. Esteban (San Francisco: ASP), 61
Puls, J., Springmann, U., & Lennon, M. 2000, A&AS, 141, 23
Santolaya-Rey, A. E., Puls, J., & Herrero, A. 1997, A&A, 323, 488
Schild, H., Crowther, P. A., Abbott, J. B., & Schmutz, W. 2003, A&A, 397, 859
Smartt, S. J., Crowther, P. A., Dufton, P. L., Lennon, D. J., Kudritzki, R. P., Herrero, A., McCarthy, J. K., & Bresolin, F. 2001, MNRAS, 325, 257
Springmann, U., & Pauldrach, A. W. A. 1992, A&A, 262, 515
Taresch, G., et al. 1997, A&A, 321, 531
Trundle, C., Dufton, P. L., Lennon, D. J., Smartt, S. J., & Urbaneja, M. A. 2002, A&A, 395, 519
Urbaneja, M. A., Herrero, A., Bresolin, F., Kudritzki, R. P., Gieren, W., & Puls, J. 2003, ApJ, 584, L73
Venn, K. A., et al. 2001, ApJ, 547, 765
Venn, K. A., McCarthy, J. K., Lennon, D. J., Przybilla, N., Kudritzki, R. P., & Lemke, M. 2000, ApJ, 541, 610
Venn, K. A., Tolstoy, E., Kaufer, A., & Kudritzki, R. P. 2004, in Carnegie Observatories Astrophysics Series, Vol. 4: Origin and Evolution of the Elements, ed. A. McWilliam & M. Rauch (Pasadena: Carnegie Observatories, http://www.ociw.edu/symposia/series/symposium4/proceedings.html)
Venn, K. A., Tolstoy, E., Kaufer, A., Skillman, E. D., Clarkson, S. M., Smartt, S. J., Lennon, D. J., & Kudritzki, R. P. 2003, AJ, 126, 1326
Vink, J. S., de Koter, A., & Lamers, H. J. G. L. M. 2001, A&A, 369, 574
Walborn, N. R., Howarth, I. D., Lennon, D. J., Massey, P., Oey, M. S., Moffat, A. F. J., & Skalkowski, G. 2002, AJ, 123, 2754